Hawassa University Journals

Volume III
Pages: 99-115
Article Number: 1095-Article Text-5988-1-4-20240429

www.journals.hu.edu.et/hu-journals/index.php/ejet/index

Ethiopian Journal of Engineering and Technology

Quantitative 3D Landslide Susceptibility Assessment Using Finite Difference Method in Hawassa City, Southern Ethiopia

Bereket Bezabih[1*], and Natnael Berded[2]

[1]*Hawassa University, Institute of Technology, Department of Civil Engineering*
bereket.bezabih@hu.edu.et

[2]*Hawassa University, Institute of Technology, Department of Civil Engineering*
natimanb326@gmail.com
**Correspond Author*

Abstract: Rapid urbanization is forcing settlement expansion to previously uninhabited areas which are potentially susceptible to geo-hazards such as landslides. Residents have moved to the foothills of Alamura Mountain in the last few decades. As a result, it is pertinent to evaluate the potential vulnerability of these settlements to landslide hazard. A three-dimensional finite difference model was developed to compute the factor of safety against rainfall triggered landslide using FLAC3D's strength reduction algorithm. The models consisted of the rock mass layer and soil layer which were generated using SRTM 30 m DEM and AI generated spatially distributed depth to bed rock (DTB) data sets. Input parameters were estimated from field and laboratory testing and correlation equations for a mohr-coulomb constitutive model. The results show the factor of safety reduces from 1.84 in dry condition to 1.0 for saturated condition with water at the surface level. The model is limited to pore pressure at grid points and no seepage pressure is used due to unfavorable zone conditions. The results show significant reduction in factor of safety and implies these settlements are susceptible for landslides. A contour map of factor of safety were generated to depict the special variation of the landslide hazard.

Key words: slope stability, strength reduction method, FLAC3D, factor of safety

Introduction

Despite the prevailing perception that landslides occur in mountainous areas with steep slopes, they are known to occur in all terrains including underwater (Highland & Bobrowsky, 2008). The rate of occurrence depends on the favorability of the region for landslides. A region's topography, climate, river course, existence of seismic activity, wild fires, and anthropogenic interventions such as clearing of vegetation cover, slope modification highly associated with a higher frequency of landslide occurrence.

In analysis of slope in stability the two major natural triggering factors are rainfall and earthquake. Anthropogenic loading of the slope due to hillside settlements and slope undercutting due to construction of infrastructure such as roads are major contributors too. Between 1980 and 2018 an estimated number of global rainfall-triggered landslide events is in the order of 15,000,000 with the average incident per year about 400,000, (Redshaw & Bottomley, 2020). Intense rainfall tends to produce shallow and quick, translational flow type landslides. Successive and prolonged rainfall stimulates deep-seated and slow landslides, (Rodriguez, et al., 2006).

Redshaw & Bottomley (2020) estimate the average annual earthquake-triggered landslide event, in the same time span, is 130,000. Spatial distribution of earthquake-induced landslides strongly correlates with distribution of volcanic tuff, (Rodriguez, 2006). Other suspect lithologies include residual, lacustrine, deltaic and costal deposits. Rock falls originating from slopes steeper than 40^{o} are the most common type of landslides, where applicable. Liquefaction is a distinct possibility along waterfronts, (Rodriguez, et al., 2006).

In Ethiopia, with 44% of the land-area classified as highland and supporting 60% of the population, there is significant risk associated with landslides. According to (GFDRR, 2019), 1% of the total land-area is classified as high landslide hazard and 18-30% medium to high landslide hazard. Redshaw & Bottomley (2020) estimated average annula number of significant landslide triggred by earthquake and rainfall in Ethiopia as 20 and 2400 respectively.

Alamura is one of the hills (highest point 2020 m a.m.s.l) on the southern end of Hawassa town, which interrupts an otherwise flat valley floor terrain on which the city lays. The rapid population growth of the town caused expansion of settlements and infrastructure development to the hills foot, which was uninhibited for most of its history, Figure 1. The hill is characterized by high slope angles on the east side and relatively mild slope on the west. The soil depth is anticipated to be shallow i.e. less than 10 m.

(a) (b)

Figure 1 Settlement pattern in Alamura Google Earth Date (a) 2003 G.C. (b) 2021 G.C.

A visual inspection of the hillsides reveals existence of relic landslides. Relict landslides are evidences of land sliding potential as existing soil mass may be supported on residual shear strength of the soil.

The Main Ethiopian Rift Valley is one of the most seismically active regions in the country hence there exists a high probability of earthquake triggered landslide. The Hawassa city and its surrounding region enjoy annual rainfall in the order of 1000 mm. Occurrence of high intensity rainfall could potentially cause rainfall induced shallow landslide event.

The risk from landslides can be assessed through estimation of the hazard, vulnerability and element at risk as $Risk = Hazard \times Vulnerability \times Element\ at\ Risk$. In the absence of element at risk, landslide event on its own will have little significance. The aforementioned rapid growth in population and infrastructure development has significantly altered the paradigm. Hence, due attention for the potential hazard, its assessment and management is timely. The present work attempts to address the first step in risk assessment, which is hazard assessment as described in the risk description above.

The general objective of this work is to determine the landslide susceptibility of Alamura Mountain in Hawassa City using 3D numerical slope stability analysis

The specific objectives of the work are:

- Develop a 3D numerical model for slope stability analysis
- Conduct pit excavation & secondary data for sample collection and validation of soil depth to bed rock (DTB) data
- Conduct field & laboratory tests to determine index and engineering properties of soils and rocks
- Determine the factor of safety against rainfall triggered slope instability using strength reduction algorithm

The work presented here covers rainfall triggered slope instability. However, the computation does not include pore water pressure due to seepage forces. The natural terrain is modeled using relatively course resolution due to computational limitation. A single soil and rock parameters are adopted.

Materials and Methods

Description of the Study Area

Hawassa is a lakeside city located some 270 km south of the national capital Addis Ababa and serves as administrative seat for Sidama regional states. With estimated total population in excess of 300,000 and rapidly

Hawassa University Journals

Volume III
Pages: 99-115
Article Number: 1095-Article Text-5988-1-4-20240429

www.journals.hu.edu.et/hu-journals/index.php/ejet/index

Ethiopian Journal of Engineering and Technology

growing, the city is a hub for social institutions such as higher education, health facilities and industrial activity, see Figure 2.

Hawassa city is located in Main Ethiopian Rift Valley (MER). It is built on Early Pleistocene Hawassa Caldera and the shades of two silicate volcanoes emerging from the floor of Middle Pleistocene Corbetti caldera, (Rapprich, et al., 2018). Early Pleistocene Hawassa ignimbrites are the oldest rocks cropping out in the area of the Hawassa. Middle Pleistocene Corbetti ignimbrites, post-caldera volcanic rocks, and non-volcanic sediments overlay these ignimbrites. A belt of basaltic rocks composed of scoria- and tuff-cones and basaltic lavas emitted from the cones transacts the Hawassa Caldera (Rapprich, et al., 2018). The Hawassa area is known for its tectonic activity by virtue of its location in MER.

Thick accumulations of unconsolidated sediments and re-sediment pyroclastics fill the Hawassa Caldera. Such a setting has the potential to amplify seismic effects during earthquakes in the wider surroundings.

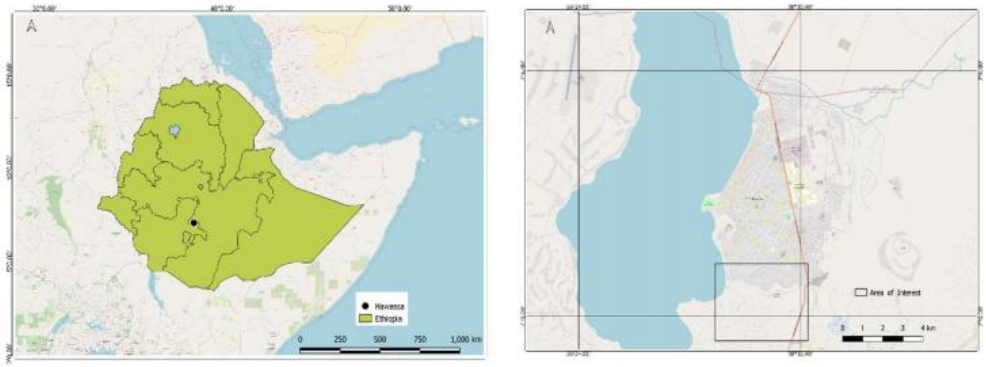

Figure 2 Location Map of Study Area (OpenStreetMapContributers, 2023)

Study Design

A 3D numerical model of the Alamura Mountain, which is located the southern end of the town, was developed. The geometric data set in stereolithographic file (STL) file used for the generation of zones in FLAC3D is prepared using GIS tools and imported to the finite difference software.

Site investigation to establish the geological and geotechnical features of the site is conducted, along with excavation of pits to validate soil depth data. In situ testing and laboratory tests on samples collected from a pit were undertake to determine index properties, strength and stiffness characteristics of the soil and rock.

The model computes in two stages. Initially, the model shall be solved to reach equilibrium. Factor of safety analysis using strength reduction method (SRM) shall be conducted with a new water level defined to be at the surface to simulate fully saturated condition.

Methods

A. Topographic Data

Digital elevation model (DEM) from SRTM 30m is clipped to a 4.6 km by 3.6 km extent of the area of interest shown in Figure 4 and used to determine the terrain of the site. The data is converted to STL file format, which can be imported into FLAC3D to generate zones and other models such as water surface. The elevation at the site, within the area of interest, ranges between 1692 m to 2020 m above mean sea level.

B. Soil Depth

Shangguan, et al., (2017) developed a global depth to bedrock data set which can be used for earth system modeling using global observation (from ca. 130,000 locations) and borehole data (ca. 1.6 million locations) using artificial intelligence techniques. The data set is available in 5 min, 30 sec and 7.5 sec resolution in TIFF file format (Dai, 2021). For the project area the depth of soil ranges between 0 – 9 m. Depth values are validated from field data collection (i.e. secondary information from local excavations) and field exploration borings. The data sampled for the study area is presented in Figure 3 (b)

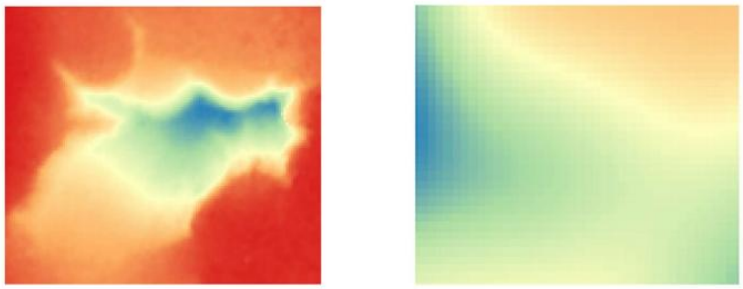

Figure 3 a) SRTM 30 m DEM for the Area of Interest (b) Depth to bedrock data extracted from Global depth to bedrock data, (Dai, 2021)

The present research adopted spatially distributed depth to bedrock (DTB) data in raster data format for developing the computational zones used in a numerical model. The data set is adopted from global data developed by (Shangguan, et al., 2017). Although the data has been validated by the team, it need to be verified for use in the area of interest.

Spatially distributed data such as the present data is ideally validated by ground truth activities i.e. conducting pit excavation at location spread over the area. In practice such an effort is time consuming and expensive. As a result, the authors attempted to take advantage of existing information on excavation of pits for the purposes of groundwater well, pit latrine etc.

A field data on depth information of wells and pit latrines were collected from 332 households in the project area. Figure 4 depicts the geolocation from which pit latrine depth data is collected. The data collection is limited by the location of settlement.

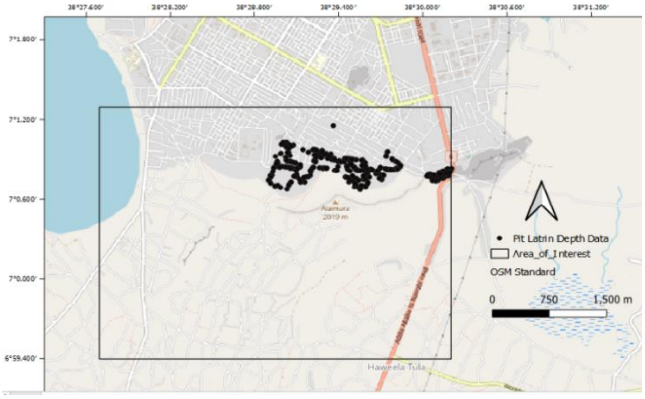

Figure 4 Location Map for Pit Latrine depth data collection

C. Site Investigation

Pit excavation was undertaken within the area of interest to establish pertinent index and engineering properties. The number of pit excavation was limited by the fact that the area is largely settled and any excavation required permission from local authorities and the cost of undertaking excavation. The site selected for excavation is located at $7^o1'1'N$ and $38^o29'46''E$. The pit has 1.5 m by 1.5 m cross section and sunk to a depth a depth of 5.2 m. Figure 5 depicts partial scenes at the excavation site.

Hawassa University Journals

Volume III
Pages: 99-115
Article Number: 1095-Article Text-5988-1-4-20240429

www.journals.hu.edu.et/hu-journals/index.php/ejet/index

Ethiopian Journal of Engineering and Technology

Figure 5 Partial Scene sat pit excavation site

A walkover survey of the project area has revealed the soil in the area of interest is largely uniform. The pit excavation revels there no significant stratification of the soil to the excavated depth.

Field density tests were conducted using core cutter method at depths 0.5 m, 1.5 m and 3.0 m depths, along with natural moisture content. Dynamic Cone Penetration (DCP) ASTM D 6951 tests were undertaken over a range of 0.4 - 1.4 m, 1.4 – 2.4 m, 2.4 -3.4 m and 5 – 6.0 m. Disturbed samples were collected for index property testing. These tests include specific gravity, particle size analysis and Atterberg's limit where applicable.

Rock samples from the site were collected and a 15 cm cube block was prepared to conduct uniaxial compressive strength test. Samples were also collected for density measurement.

Analysis

A. Determination of Parameters for Soils and Rock Mass

The following equations were put forward by (Mohammadi, et al., 2008) for correlation between relative density, Young's Modulus and total and effective internal angle of friction.

Table 1 Correlation Equation as per (Mohammadi, Nikoudel, Rahimi, & Khamechiyan, 2008)

Parameter	Equation	Correlation R^2
Relative Density,%	$D_r = 189.93(DCPI)^{-0.532}$	$R^2 = 0.9851$
Young's Modulus, MPa	$E = 55.033(DCPI)^{-0.5459}$	$R^2 = 0.8272$
Internal Angle of Friction, Deg.	$\phi' = 52.16/(DCPI)^{0.13}$	$R^2 = 0.9$

Rapprich & Hroch (2014) compiled a 1:50,000 geology map of the study area which reports the Alamura Mountain as rhyolitic ignimbrite lower Pleistocene. These rocks were produced by voluminous eruptions of a rhyolitic magma from the Hawassa Caldera. The rock mass is intensely jointed and faulted. Crystaloclasts of quartz and feldspars can be identified enclosed in a groundmass of deformed glass shards and frequent fiamme. The geological strength index (GSI) is used to determine the parameters of the rock mass.

Figure 6 A photograph of a rock mass near the site

The rock mass strength, σ_{cm}, cohesion c_m and friction ϕ_m are computed using Hoek- Brown parameters$s$, a and m_b.

The deformation properties of a rock mass can be estimated from the uniaxial compressive strength of the intact rock (Hoek & Diederichs, 2006), (Palmstrom & Singh, 2001).

$$E_{rm}(MPa) = E_i \left[0.02 + \frac{1-(D/2)}{1+e^{((60+15D-GSI)/11)}}\right] \quad (1)$$

$where$	$E_i = MR * \sigma_{ci}$
E_i	Deformation Modulus of Intact Rock
MR	Modulus Ratio
σ_{ci}	Uniaxial Compressive Strength (MPa)
D	Disturbance Factor
GSI	Geological Strength Index

The shear and bulk moduli are computed from the Young's modulus values for assumed Poisson's ratio 0.2 and 0.25 using elasticity equations as,

$$K = \frac{E}{2(1+\nu)} \quad \& \quad G = \frac{E}{2(1-2\nu)} \quad (2)$$

$$m_b = m_i e^{\left(\frac{GSI-100}{28-15D}\right)} \quad (3)$$

$$s = e^{\left(\frac{GSI-100}{9-3D}\right)} \quad (4)$$

$$a = \frac{1}{2} + \frac{1}{6}\left(e^{\frac{-GSI}{15}} - e^{-\frac{20}{3}}\right) \quad (5)$$

$$\sigma'_{cm} = \sigma_{ci} \frac{(m_b+4s-a(m_b-8s)(m_b/4+s)^{a-1}}{2(1+a)(2+a)} \quad (6)$$

Hawassa University Journals

Volume III
Pages: 99-115
Article Number: 1095-Article Text-5988-1-4-20240429

www.journals.hu.edu.et/hu-journals/index.php/ejet/index

Ethiopian Journal of Engineering and Technology

$$\frac{\sigma'_{3max}}{\sigma'_{cm}} = 0.72\left(\frac{\sigma'_{cm}}{\gamma H}\right)^{-0.91} \quad \& \quad \sigma_{3n} = \frac{\sigma_{3max}}{\sigma_{ci}} \qquad (7)$$

$$c_m = \frac{\sigma_{ci}[(1+2a)s+(1-a)m_b\sigma_{3n}](m_b\sigma_{3n}+s)^{a-1}}{(1+a)(2+a)\sqrt{1+(6am_b\sigma_{3n}+s)^{a-1}/(1+a)(2+a)}} \qquad (8)$$

$$\phi_m = sin^{-1}\left[\frac{3am_b(m_b\sigma_{3n}+s)^{a-1}}{(1+a)(2+a)+3am_b(m_b\sigma_{3n}+s)^{a-1}}\right] \qquad (9)$$

B. Numerical Model

Numerical modeling in FLAC3D begins with generating zones. For an irregular natural terrain such as Alamura, the required zones can be generated from geometry data sets. For Alamura slope stability analysis, an SRTM 30m DEM is used to generate a geometric set same 'surface' (STL), The depth to bed rock (DTB) data set is subtracted from the DEM data set using raster algebra in QGIS to produce the lay out for 'bed rock' (STL).These geometry sets are imported and used to generate zones in FLAC3D. A 'Base' layer of zones is sued to control the zone densities and subsequent two sets of zones were generated each representing the bedrock 'Weathered Rock Layer' and the surface 'Soil Layer' respectively at the area of interest. Figure 7 shows the geometry set which shall be used to generate zones.

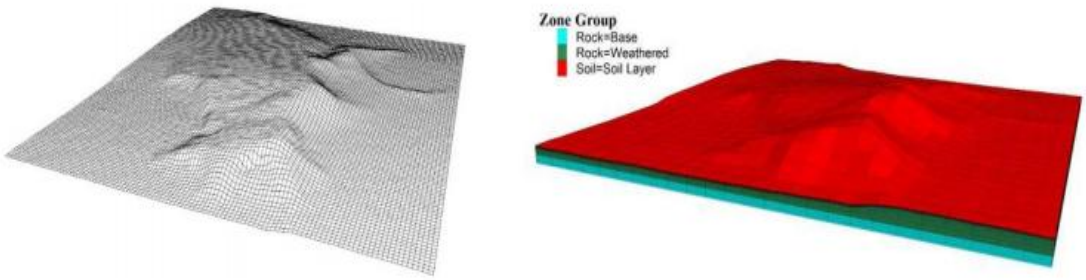

Figure 7 Numerical Model geometric layer and computation zones

The conditions of the resulting zones, as measured by built in metrics such as volume ratio, orthogonality and face planarity, falls the ideal state. The major problem that results from these self-intersecting, zero or negative volume zones is that they cannot model fluid flow. The proportion of problematic zones decreases with increased resolution of zones. However, the added number of zones will result lower computation speed. For Alamura slope stability analysis model, the doubling the resolution in x and y directions from 120 x 110 to 240 x 220 and 480 x 440 improved the proportion of high quality zones to 84%, 93.6 % and 98.1% respectively. These zone densities require significant computation time. As a result the final computation is done using zone density for the base layer 30 x 25 x 3 which generates 13500 zones.

C. Constitutive Models

Mohr-Coulomb (elastic perfectly plastic model) shall be adopted for the soil mass and the rock mass. The failure envelope for this model corresponds to a Mohr-Coulomb criterion (shear yield function) with tension cutoff (tension yield function). The strength reduction algorithm applies only on plastic models.

D. Factor of Safety Analysis

Factor of Safety (FOS) analysis is conducted to determine the areas of the terrain susceptible to slope failure. In strength reduction algorithm, successive trial factor of safeties are selected and applied to the strength parameters until the soil/rock material yields. For a Mohr-coulomb (c, ϕ) material the equations of strength reduction method are given as follows;

$$c^{trial} = \frac{c}{F^{trial}} \quad (10)$$

$$\phi^{trial} = \arctan\left(\frac{\tan\phi}{F^{trial}}\right) \quad (11)$$

After the model is solved to generate initial stress states, the factor of safety computations continues for various potential slope failure trigger events, such as surcharge loads, rainfall, earthquake etc. In this work, the triggering event is rainfall. The rainfall event is simulated by generating pore-water pressure within the model by assuming water level at the ground surface. A full-fledged coupled analysis accounting for groundwater flow (including seepage forces) is not modeled in here. The main reason being the zones generated from the natural irregular geometry continue to have a self-intersecting region resulting in negative or zero volume zones.

Results and Discussions

Results

A. Validating DTB Data Set

The well and pit latrine depth data collected using KOBO Tool Box was analyzed to validate the AI generated DTB data. The average reported depth of excavation is 5.9 m. Some 150 respondents (45 % of surveyed households) reported excavation stopped due to existence of rocky materials with an average depth 4.6 m. The mean depth over the area interest from the AI generated data is 6.02 m, with a minimum and maximum depth of 0.3 m and 10.7 m respectively.

The discrepancy between result of the survey and the AI generated can partially be explained by the large sample over flatter terrain where the depth of soil can be larger as opposed to the surveyed data which is confined to settlement along the steep slope.

B. Filed Tests Results

The results of field density test are presented in Table 1. The relatively low-density values are typical for volcanic deposits such as the case for Hawassa caldera.

Table 1 Field Bulk Density, Natural Moisture Content and Dry Density at Various Depths

Sample Depth	**0.5 m**	**1.5 m**	**3 m**
Bulk Density $(\boldsymbol{g/cm^3})$	1.2	1.2	1.1
Water content, %	9.0	8.2	11.5
Dry Density $(\boldsymbol{g/cm^3})$	1.1	1.1	1.0
Void Ratio	1.10	1.08	1.56
Saturated Density $(\boldsymbol{g/cm^3})$	1.17	1.18	1.08

Dynamic cone penetration test (DCP) results are shown in the Figure 8. The gap in the data between 3.4 m to 5.0 m is caused by logistical reasons. The observed soil excavated from these missing range shows no marked difference in physical attributes, As a result no significant variation expected from measured section of the pit.

Furthermore the mean value over the corresponding depth is used in correlation to establish pertinent values for parameters such as Young's Modulus,E internal angle of friction,ϕ and relative density. For the purposes of the current work correlation equations developed by (Mohammadi, et al., 2008) for soil engineering properties of sandy soils is adopted. The average values of DCPI values are various depths were computed.

Hawassa University Journals

Volume III
Pages: 99-115
Article Number: 1095-Article Text-5988-1-4-20240429

www.journals.hu.edu.et/hu-journals/index.php/ejet/index

Ethiopian Journal of Engineering and Technology

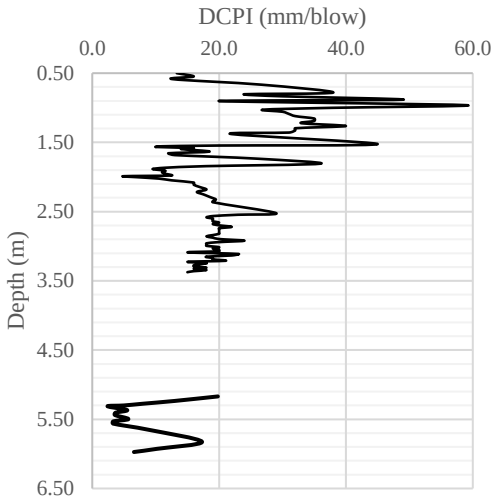

Figure 8 Result of DCP test at the pit excavation site

Table 2 Correlation between DCPI and Soil Parameters

Depth (m)	DCPI (mm/ blow)	Young's Modulus (MPa)	Internal Angle of friction φ' (deg)	Internal Angle of friction φ (deg)
1.4	29.7	4.3	33.6	32.7
2.4	16.8	6.6	36.1	34.4
3.4	17.2	6.5	36.0	34.3
5.4	9.5	10.1	38.9	36.6
Mean		6.9	36.2	34.5

C. Laboratory Test Results

Disturbed samples were collected for index property testing. These test include specific gravity, particle size analysis and Atterberg's limit where applicable.

Particle size analysis was conducted on samples collected at various depths. The result of the analysis is plotted on Figure 3-2. All soil samples have less than 2 % passing sieve no 200 (0.075 mm) hence predominantly sandy. The USCS classification of classify the soils as poorly graded sand, SP.

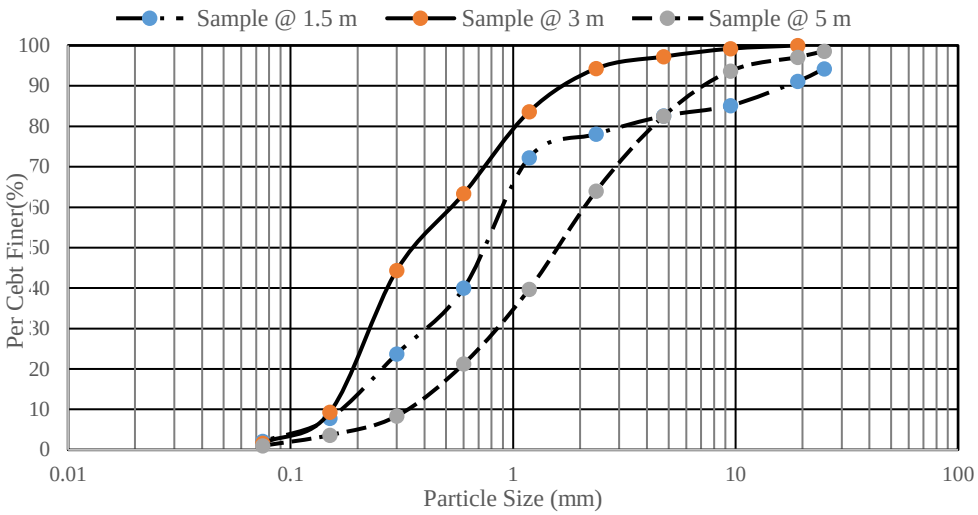

Figure 9 Particle Size Distribution of Soil Samples from Pit Excavation

Compressive Strength Test on a 15 cm cubic rock sample was conducted. The average compressive strength of samples is 15.1 MPa. In order to implement the certain rock mass properties need to be adopted. These are based on observation of the rock mass, the type of the intact rock mass etc. These value are summarized in Table 5.

Table 3 Parameters Used in Numerical Model

Description	Base Layer	Weathered Rock	Soil Layer	Remark
Compressive Strength, $\boldsymbol{\sigma_{ci}(MPa)}$	15.1	15.1	N/A	
Rock Modulus	400	400	N/A	
HB Parameter $\boldsymbol{m_i}$	20	20	N/A	
GSI	40	25	N/A	
Unit Weight $\boldsymbol{\gamma}$ $\boldsymbol{(kN/m^3)}$	20	19	11.43	
Young's Modulus, E (MPa)	964.3	364.5	6.9	
Poisson's Ratio, $\boldsymbol{\nu}$	0.2	0.25	0.3	Assumed
Bulk Modulus, K (MPa)	803.6	361.5	8.6	
Shear Modulus, G (MPa)	401.8	145.6	2.7	
Friction, $\boldsymbol{\phi}$ (Degrees)	42	39.8	34	
Cohesion $\boldsymbol{c}$, (kPa)	398.3	234.5	100*	

* Assumed value to facilitate faster convergence

The cohesion values given above computed using as equivalent from Hoek-Brown parameters are upper bound values. The cohesion value adopted for the soil is not a measured value but a value to facilitate computational efficiency in the model. The Mohr-Coulomb model requires a tension limit value. The model adopts the provided value if it is less than $c/\tan\phi$.

D. Factor of Safety

Factor of safety analysis was conducted for two scenarios. The first scenario depicts 'dry' condition, i.e. without development of pore water pressure at grid points. The second scenario depicts 'wet' condition, i.e. with pore pressure development at grid points. For the 'wet' condition the water surface is assumed to be at the surface level.

For the 'dry' condition the computed minimum stable factor of safety is 1.84. Figure 10 shows the plan view the area which would for a higher factor of safety than 1.84.

Hawassa University Journals

Volume III
Pages: 99-115
Article Number: 1095-Article Text-5988-1-4-20240429

www.journals.hu.edu.et/hu-journals/index.php/ejet/index

Ethiopian Journal of Engineering and Technology

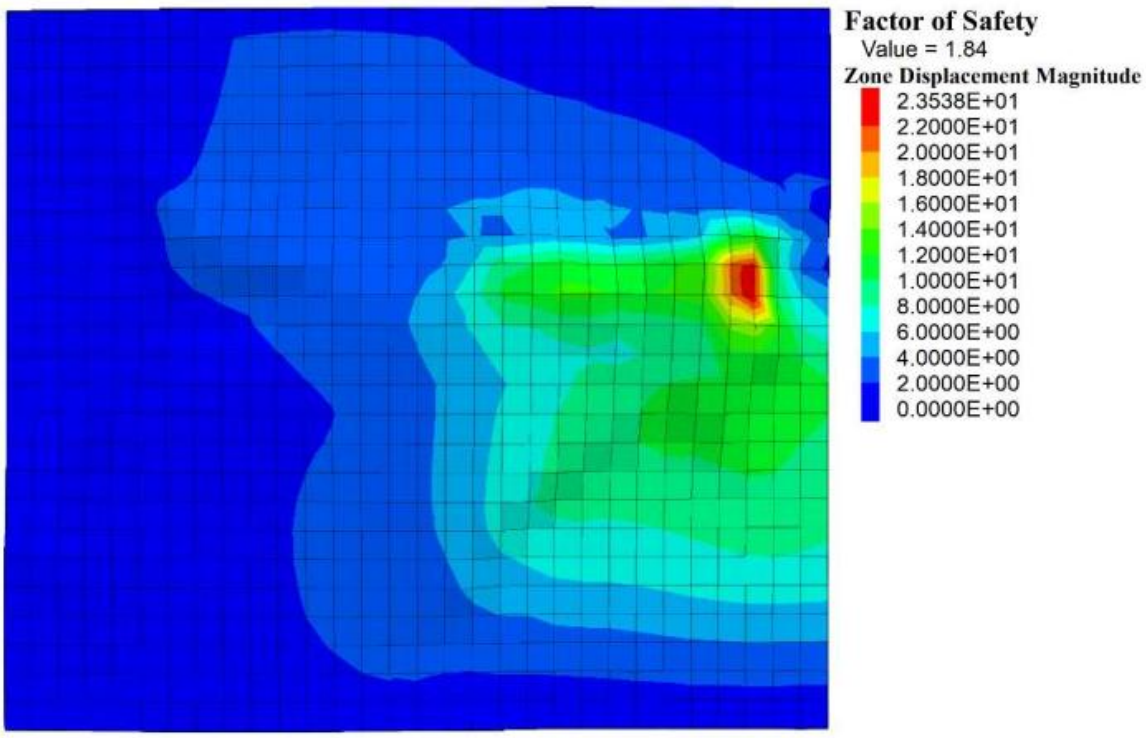

Figure 10 Factor of Safety 'dry' condition

FLAC3D is capable of plotting a contour map of factor of safeties and the location which will be affected by a higher factor of safety values as shown in Figure 11.

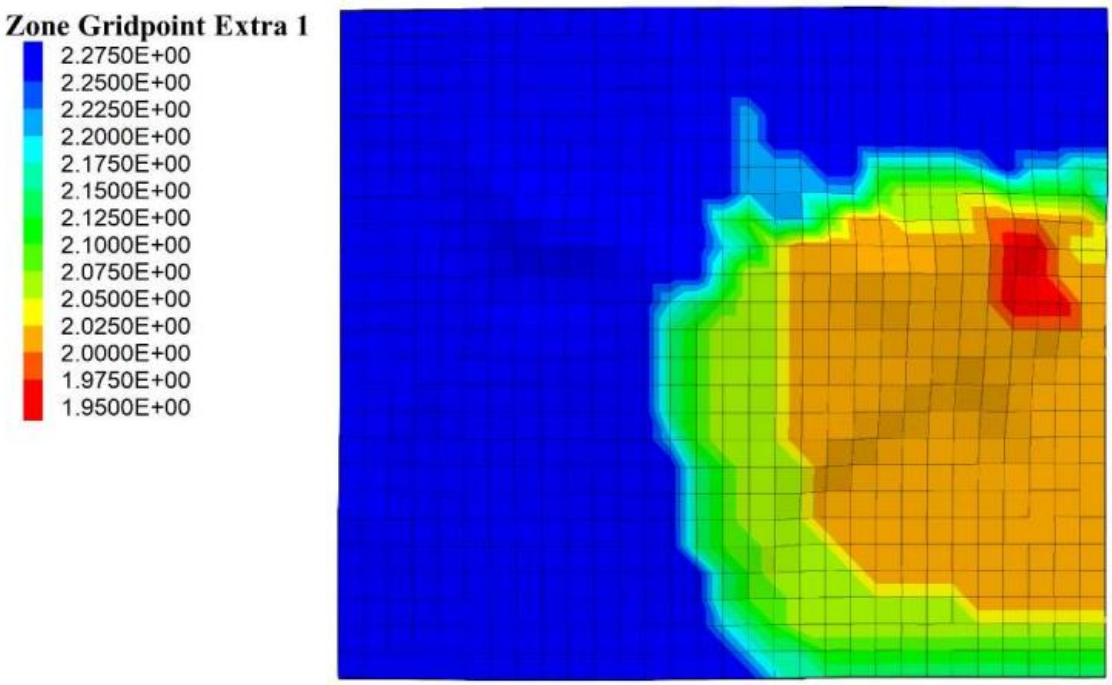

Figure 11 Factor of Safety Contour for dry Condition

For the 'wet' condition the computed minimum stable factor of safety reduces to 1.0. Figure 12 shows the location susceptible movement for factor of safety values higher than 1.0.

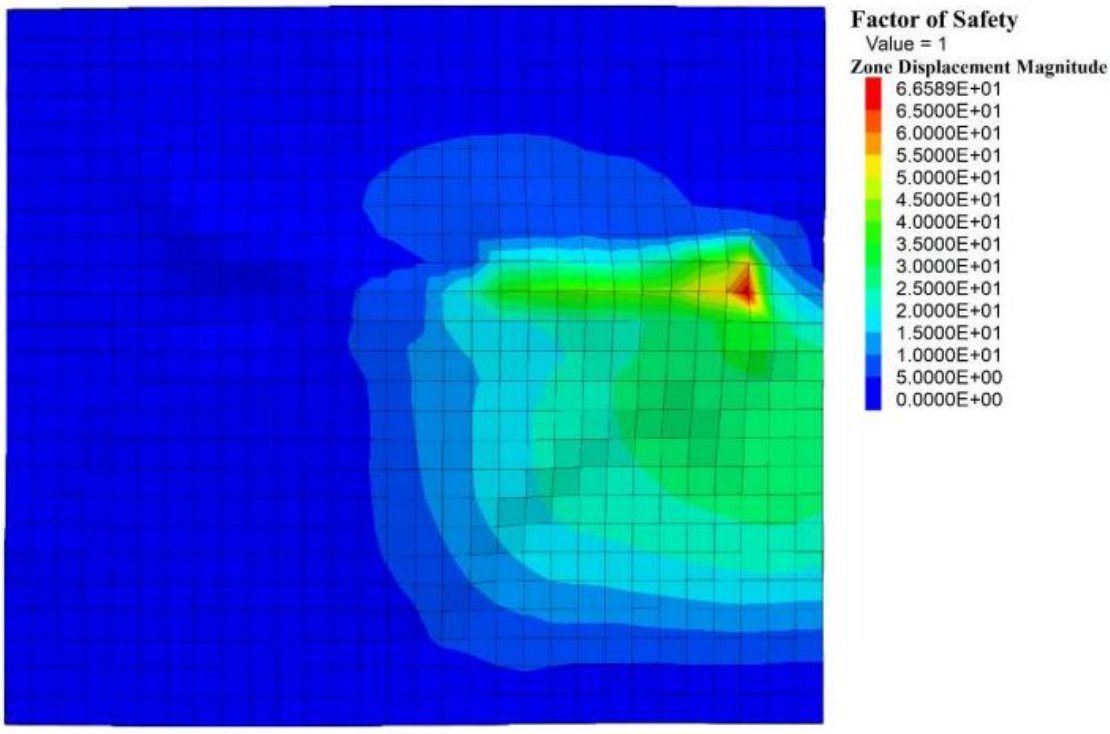

Figure 12 Factor of Safety for 'wet' condition

The contour plot of factor of safeties in 'wet' condition is depicted on figure 12.

Hawassa University Journals

Volume III
Pages: 99-115
Article Number: 1095-Article Text-5988-1-4-20240429

www.journals.hu.edu.et/hu-journals/index.php/ejet/index

Ethiopian Journal of Engineering and Technology

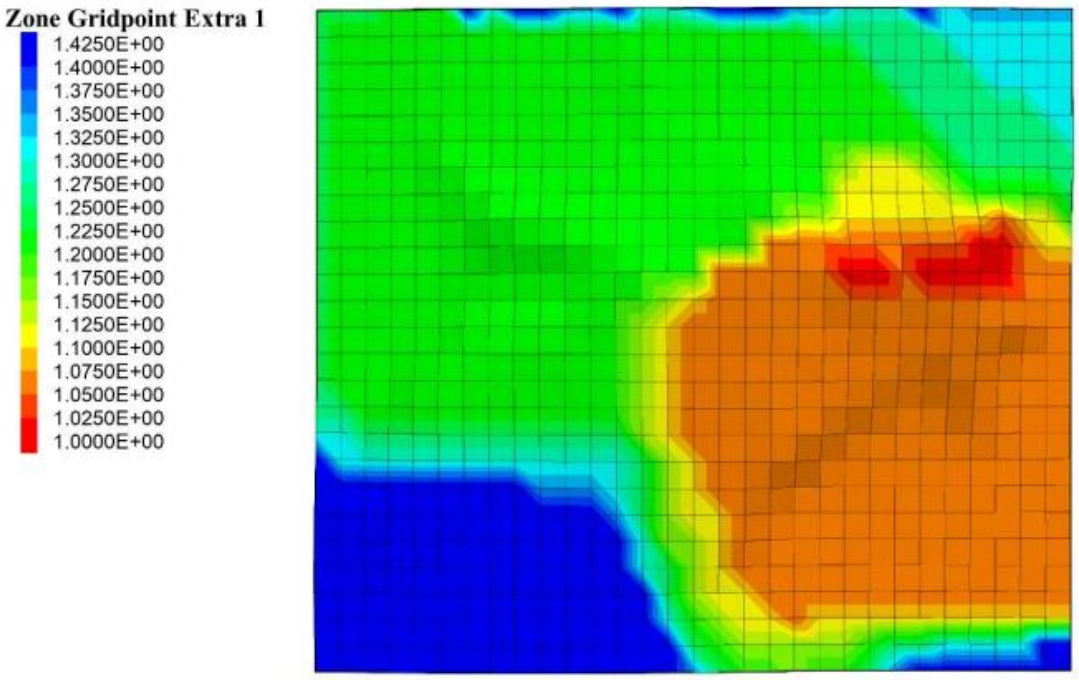

Figure 13 Factor of Safety contours for 'wet' condition

Discussion

The AI generated data set represents the DTB at the area interest fairly adequately. However, the validation is based on secondary data sources and a single pit excavation. As a result, any further use of the data set needs independent verification of larger scale.

The adopted correlation equation between DCPI and the various soil parameters are based on the fact that the soils for which the equations were derived for and the soils in the field belong to the same USCS group of poorly graded sand, SP.

The parameters adopted for the rock mass properties such as the Rock Modulus (MR), Hoek-Brown parameter (m_i) are based on the intact rock type of rhyolitic ignimbrite. The value of GSI depends on the intensity of discontinues provided on literature and physical inspection of the rock mass.

The use of large number of zones improves the zone quality in the model. However, the computation time required will grow above manageable level. As a result, a low density mesh 30 x 25 x 3 for the base layer is adopted reducing the number of zones to 13500. This is expected to have impact on the accuracy of the final result.

The 'wet' condition described above generates pore pressure at each node with water surface assumed to be at ground level. It is used to simulate rainfall triggered slope failure. However, the computation does not include seepage pressure developed during such natural event. This is because of low zone quality caused by low density zones.

The factor of safety algorithm in FLAC3D 6.0 does not apply to elastic constitutive models. As a result, both the rock mass and the soil were modeled using elastic- plastic mohr-coulomb model. The maximum potential displacement aligns with the maximum slope location on the terrain, which is the East/North East side of the mountain. It is worth noting a separate shallow depth analysis limited to the overlaying soil mass (excluding the rock mass) the location of maximum strain may differ from the result in the present analysis.

Conclusions and Recommendations

Conclusions

The minimum stable factor of safety computed for 'dry' condition and 'wet' conditions are 1.84 and 1.0 respectively. The location of the material susceptible movement is located on the south side of Alamura Mountain. In the wet condition, there is an impending motion.

The contour maps for the 'wet' condition shows larger area will be susceptible to movement as compared to the 'dry' condition. The large majority of population settlement exists on the north side of the mountain where the factor of safeties are higher for both 'dry' and 'wet' conditions.

The strength reduction algorithm in FLAC3D does not apply on 'elastic' model. As a result, separate analysis of the relatively weak soil material was not possible. Shallow slope failure contained within the soil mass may occure prior to the movement computed in this work.

The use of one DTB data sets limits the ability to incorporate a varied parameter values in different parts of the problem domain. Hence, a separate DTB data sets are required and merged during geometry generation. Otherwise the approach shall be limited to slopes of fairly uniform soil types.

Computational efficiency is a major factor in deterring determination of accurate factor of safety values. It is affected by zone density and cohesion parameter values.

Recommendations

The computation shall be done with a higher density zones with a complete fluid flow model, which require higher computational capacity to establish a more accurate factor of safety maps. The condition characterized as 'wet' does not account for seepage forces. Only pore pressure values resulting from hydrostatic pressures defined by a water surface geometry are accounted for in the analysis.

Slope instability can be triggered by factors other than rainfall, which include anthropogenic activities and earthquakes. For a 'complete' factor of safety, dynamic analysis shall be conducted to determine the factor of safety against earthquake triggered landslides. This is highly pertinent as Hawassa is located within the Main Ethiopian Rift Valley (MER).

Although the analysis result for the 'wet' condition implies impending movement, real world slopes are complicated than the numerical model considered here and existing slope with no movementare assumed to be safe enough. Hence shall need no immediate intervention.

Quantitative stability analysis, such as the one presented here, can be repeated in other areas where there is risk to lives and properties using the model developed in the present project. The only additional information required shall be the terrain geometry sets and material properties.

References

Brabb, E. E., 1991. The World Landslide Problem. Episodes, Vol (14) No (1), pp. 52-62.

Dai, Y., 2021. Global Map of Depth to Bedrock. [Online] Available at: http://globalchange.bnu.edu.cn/ or http://soilgrids.org/.

GFDRR, 2019. Disaster Risk Profile,Ethiopia, Washington D.C.: World Bank Group.

Highland, M. & Bobrowsky, P., 2008. The Landslide Handbook,a guide to Understanding Landslides. Reston(Virginia): USGS.

Hoek, E. & Diederichs, M., 2006. Emperical Estimates of Rock Mass Modulus. Int. J. Rock Mech. Min. Sci., Volume 43, pp. 203-205.

JICA, 2012. Geological Map of Sodo-Aawassa Area, s.l.: JICA.

Mohammadi, S., Nikoudel, M., Rahimi, H. & Khamechiyan, M., 2008. Appilcation of Dynamic Cone penetrometer (DCP) for Determination of the Engineering Properties of Sandy Soils. Engineering Geology, Volume 101, pp. 195-203.

OpenStreetMapContributers, 2023. OSM. [Online] Available at: Planet dump [Data file from $date of database dump$]. Retrieved from https://planet.openstreetmap.org [Accessed December 2023].

Palmstrom, A. & Singh, R., 2001. The Deformation Modulus of Rock Masses; Comparisions between Insitue Tests and Indirect Estimates. Tunnelling and Underground Space, Volume 16, pp. 115-131.

Rapprich, V. & Hroch, T., 2014. CGS. [Online]
Available at: http://www.geology.cz/projekt681700/vystupy
[Accessed 01 05 2022].

Rapprich, V. et al., 2018. Hawassa Subsheet, Addis Abeba: Czech Geological Survey,Geological Survey of Ethiopia.

Redshaw, P. & Bottomley, J., 2020. The global landslide Hazard Map, London UK: ARUP & Partners International Ltd, World Bank Group.

Rodriguez, C. E., 2006. Earthquake-Induced Landslides:Central America Geology Resources and Hazards. Buldschuh and Alvarado ed. s.l.:Balkema.

Rodriguez, C. E., Torres, A. T. & Leon, E. A., 2006. Landlside Hazard in El Salvador. s.l., s.n., pp. 6-16.

Shangguan, W. et al., 2017. Mapping the global depth to bedrock for land. Journal of Advances in Earth Systems, pp. 65-88.

Acknowledgment

This research was funded by the Annual Disciplinary Research Funding Program of Hawassa University for the year 2015 E.C/2022/23 G.C.

Hawassa University Journals

Volume III
Pages: 99-115
Article Number: 1095-Article Text-5988-1-4-20240429

www.journals.hu.edu.et/hu-journals/index.php/ejet/index

Ethiopian Journal of Engineering and Technology

ANNEX

Edit geometry.f3dat

```
;=-----------------------------------------------------------------------------------------------------=
;=                                  Ala Mura 3D Slope Stability Analysis                               =
;=                                        Hawassa,Ethiopia                                             =
;=-----------------------------------------------------------------------------------------------------=
model new
model title 'Ala Mura 3D Slope Stability Analysis';Out put model name in plots and saves it in program file
fish automatic-creat off;Avoids automatic creation of global variables from unrecognized strings
;Creat grid & geometric set
geometry import 'bed_rock.stl'
zone creat brick size 30 25 3 ...
&                         Point 0 (441244.0,772741.0,1600.0)...
&                         Point 1 (445080.0,772741.0,1600.0)...
&                         Point 2 (441244.0,776087.0,1600.0)...
&                         Point 3 (441244.0,772741.0,1650.0)...
&                         group 'Base' slot 'Rock'
;Creat bed rock zones from geometry
zone generate from-topography geometry-set 'bed_rock'...
&                         segment 10 ratio 0.6 ...
&                         group 'Weathered' slot 'Rock'
;Creat soil layer from soil geometry
geometry import 'surface.stl'
zone generate from-topography geometry-set 'surface'...
&                         segment 5 ratio 0.4 ...
&                         group 'Soil Layer' slot 'Soil'
zone face skin slot-skin 'External'
model save 'alamura_geometry'
;Assign Constitutive Models to Groups
zone cmodel assign mohr-coulomb range group 'Base'
zone cmodel assign mohr-coulomb range group 'Weathered'
zone cmodel assign mohr-coulomb range group 'Soil Layer'
;Assign properties
zone property bulk 803.6e6 shear 401.8e6 density 2000 friction 42 cohesion 398.3e3 ...
&                   tension 440e6 range group 'Base'
zone property bulk 361.5e6 shear 145.6e6 density 1900 friction 39.8 cohesion 234.5e3 ...
&                   tension 288e6 range group 'Weathered'
zone property bulk 8.6e6 shear 2.7e6 density 1143 friction 34 cohesion 1e5 ...
&                   tension 150e6 range group 'Soil Layer'
;Apply Boundary Conditions
zone face apply velocity-normal 0 range group 'East' or 'West'
zone face apply velocity-normal 0 range group 'North' or 'South'
zone face apply velocity-normal 0 range group 'Bottom'
model step 0
;Assign Initial Condition (Stress due to Gravity)
model gravity 9.81
zone initialize-stresses ratio 0.5; ratio of horizontal to vertical stress with Poissons raio 0.3
zone list information;Lists the charachterstics of geometric zones
model solve elastic ratio-local 1e-3;reduced the convergence criteria from 1e-5 to reduce computation time for large model
model save 'initial'
```

Edit fosmin.f3dat

```
model restore 'initial'
;Solve for initial factor-of-safety
model factor-of-safety ratio-local 1e-3 filename 'fosmindry'
```

Edit fosmincontour.f3dat

```
model restore 'initial'
;Computes contours of factor of safety using FISH function
zone gridpoint initialize displacement (0,0,0)
zone gridpoint initialize velocity (0,0,0)
call 'foscontour' suppress
@FOSContours(1.8,1e-3,0.05,30000,10,[false])
model save 'FOSContours'
```

Edit foscontour.f3dat

```
fish automatic-create off

; fsmin        = Starting minimim safety factor
; vel_limit    = Threshold velocity below which a given gridpoint
;                is considered stable
; inc_fs       = Amount safety factor is increment each stage
; max_num_cyc  = Number of cycles that is taken at each stage
; t_stages     = Total stages taken - maximum safety factor is then
;                fsmin + (total-stages-1)*in_fs
; inc_tens     = If true, then tension is included in the
;                general strength reduction
fish define FOSContours(fsmin,vel_limit,inc_fs,max_num_cyc,t_stages,inc_tens)
    ; Initialize storage in zones and gridpoints
    loop foreach local gp gp.list
        gp.extra(gp,1) = 0
    end_loop
    loop foreach local zone zone.list
        zone.extra(zone,1) = zone.prop(zone,'cohesion')
        zone.extra(zone,2) = zone.prop(zone,'friction')
        zone.extra(zone,3) = zone.prop(zone,'tension')
    endloop
    ; Loop through stages of target safety factor
    local k = 0
    local numb = 0
    loop while k < t_stages
        ; Calculate safety factor for stage, and reduce cohesion, friction,
        ; and tension accordingly
        local fs = fsmin + k*inc_fs
        loop foreach zone zone.list
            zone.prop(zone,'cohesion') = zone.extra(zone,1) / fs
            zone.prop(zone,'friction') = ...
&           math.atan(math.tan(zone.extra(zone,2)*math.degrad)/fs)/math.degrad
            if inc_tens then
                zone.prop(zone,'tension') = zone.extra(zone,3)/fs
            endif
        endloop
        ;
        local num_cyl_0 = global.step
        command
            model solve cycles @max_num_cyc ratio-local 1e-3
        endcommand
        loop foreach gp gp.list
            if gp.extra(gp,1) = 0 then
                local vel = math.mag(gp.vel(gp))
                if vel > vel_limit then
                    gp.extra(gp,1) = fs - inc_fs
                endif
            endif
        endloop
        if (global.step-num_cyl_0) > max_num_cyc then
          numb = numb + 1
        endif
        k = k + 1
    endloop
    loop foreach gp gp.list
        if gp.extra(gp,1) = 0 then
          gp.extra(gp,1) = fs + inc_fs/2.0
        endif
    endloop
end
```

Hawassa University Journals

Volume III
Pages: 99-115
Article Number: 1095-Article Text-5988-1-4-20240429

www.journals.hu.edu.et/hu-journals/index.php/ejet/index

Ethiopian Journal of Engineering and Technology

Edit geometry.f3dat

```
;=============================================================================================================
;=                                    Ala Mura 3D Slope Stability Analysis                                   =
;=                                          Hawassa,Ethiopia                                                 =
;=============================================================================================================
model new
model title 'Ala Mura 3D Slope Stability Analysis';Out put model name in plots and saves it in program file
fish automatic-creat off;Avoids automatic creation of global variables from unrecognized strings
;Creat grid & geometric set
geometry import 'bed_rock.stl'
zone creat brick size 30 25 3 ...
&                     Point 0 (441244.0,772741.0,1600.0)...
&                     Point 1 (445080.0,772741.0,1600.0)...
&                     Point 2 (441244.0,776087.0,1600.0)...
&                     Point 3 (441244.0,772741.0,1650.0)...
&                     group 'Base' slot 'Rock'
;Creat bed rock zones from geometry
zone generate from-topography geometry-set 'bed_rock'...
&                     segment 10 ratio 0.6 ...
&                     group 'Weathered' slot 'Rock'
;Creat soil layer from soil geometry
geometry import 'surface.stl'
zone generate from-topography geometry-set 'surface'...
&                     segment 5 ratio 0.4 ...
&                     group 'Soil Layer' slot 'Soil'
zone face skin slot-skin 'External'
model save 'alamura_geometry'
;Assign Constitutive Models to Groups
zone cmodel assign mohr-coulomb range group 'Base'
zone cmodel assign mohr-coulomb range group 'Weathered'
zone cmodel assign mohr-coulomb range group 'Soil Layer'
;Assign properties
zone property bulk 803.6e6 shear 401.8e6 density 2000 friction 42 cohesion 398.3e3 ...
&                   tension 440e6 range group 'Base'
zone property bulk 361.5e6 shear 145.6e6 density 1900 friction 39.8 cohesion 234.5e3 ...
&                   tension 288e6 range group 'Weathered'
zone property bulk 8.6e6 shear 2.7e6 density 1143 friction 34 cohesion 1e5 ...
&                   tension 150e6 range group 'Soil Layer'
;Apply Boundary Conditions
zone face apply velocity-normal 0 range group 'East' or 'West'
zone face apply velocity-normal 0 range group 'North' or 'South'
zone face apply velocity-normal 0 range group 'Bottom'
model step 0
;Assign Initial Condition (Stress due to Gravity)
model gravity 9.81
zone water density 1000 effective
zone water set 'surface'; initialize pore pressure at grid point
zone initialize-stresses ratio 0.5; ratio of horizontal to vertical stress with Poissons raio 0.3
zone list information;Lists the charachterstics of geometric zones
model solve elastic ratio-local 1e-3;reduced the convergence criteria from 1e-5 to reduce computation time for large model
model save 'initial'
```